Photopyroelectric spectroscopy of *a*-Si:H thin semiconducting films on quartz

A. Mandelis, R. E. Wagner, K. Ghandi, and R. Baltman
Photoacoustic and Photothermal Sciences Laboratory, Department of Mechanical Engineering, and Ontario Laser and Lightwave Research Center, University of Toronto, Toronto, Ontario, Canada M5S 1A4

Phat Dao
Corporate Analytical Laboratory, Eastman Kodak Research Laboratories, Rochester, New York 14650
(Received 19 August 1988)

Photopyroelectric spectroscopy (PPES) of plasma-enhanced chemical-vapor-deposited *a*-Si:H thin films on quartz has been performed and compared with the conventional widely used photothermal deflection spectroscopy (PDS). High-modulation-frequency (thermally thick limit) data were combined to yield self-consistent optical-absorption-coefficient *and* nonradiative quantum efficiency spectra. The quality of the PPES optical-absorption-coefficient spectrum was found to be similar to the PDS spectrum. The former technique, however, has the advantage of not requiring a coupling fluid interface to the delicate, electronically active thin film.

I. INTRODUCTION

Photopyroelectric spectroscopy has proven to be a sensitive qualitative[1] and quantitative[2] technique for thin-film spectroscopic applications. An important feature of this back-surface-detection technique, not shared with the more conventional front-surface photothermal detection methods [photothermal deflection spectroscopy (PDS) and photoacoustic spectroscopy (PAS)] is its ability to measure *directly* and *separately* two independent spectrally varying parameters: the optical-absorption coefficient[3] and the nonradiative quantum efficiency. PDS of thin semiconducting films of amorphous hydrogenated Si[4] readily yields information about the *product* of the optical absorption coefficient, $\alpha(\lambda)$, and the nonradiative quantum efficiency, $\eta(\lambda)$. The standard assumption is, however, that $\eta(\lambda)$ is not a sensitive function of the exciting-photon energy. This assumption is generally wrong, and nonradiative quantum efficiencies have been found photoacoustically to vary by 1 order of magnitude[5] across the optical gap in Ge-doped As_2Se_3 chalcogenide glasses. PAS yields amorphous thin-film spectra similar to PDS.[6] The working assumption has been that PA spectra are essentially accurate above the optical gap, as $\eta(\lambda)$ is expected to be independent of photon energy. Kitamura *et al.*[5] were able to derive extended $\eta(\lambda)$ spectra of $(As_2Se_3)_{100-x}Ge_x$ glasses upon combining PA spectra with optical-absorption-coefficient information obtained in an independent spectrophotometric experiment using ordinary polished bulk samples. These authors, however, were not able to guarantee that the glasses and the bulk samples had the same (or even nearly similar) $\alpha(\lambda)$ spectra.

From an experimental point of view, it is highly desirable to develop a thin-film photothermal spectroscopic technique which can exhibit the convenience and high sensitivity of PDS without the requirement for a fluid intermediate with a large-refractive-index gradient $\partial n/\partial T$ (e.g., CCl_4), where the probe beam may propagate and get deflected. The presence of the liquid interface in PDS precludes experimentation at low temperatures and may have electrochemical consequences in the case of ultrathin quantum-well structures. In that case, alternative interface wave-guiding structures, involving the contact of the epitaxial side with a glass slide, have been employed.[7] Furthermore, in terms of detector-noise limitations, PAS suffers from microphonic acoustic noise,[8] and PDS is probe-beam-Poynting-noise limited.[8,9] PPES, on the other hand, operates on the pyroelectric principle and is not limited by the above-mentioned noise sources. Finally, in our own experience, and in that of others,[10] we have found that three-dimensional effects associated with the location of the laser probe beam with respect to the dark edge of the illuminated sample surface region in a PDS experiment have substantial influence on the PDS measurements. An alternative method which is insensitive, or less sensitive than PDS, to such geometrical constraints would appear desirable at this point in the evolution of thin-film photothermal spectroscopies.

In this work we present our preliminary findings in the first application of PPES to *a*-Si:H thin-film investigations and compare features of the obtained spectra to conventional PDS data.

II. THEORETICAL

Figure 1 shows the idealized geometry for PPES detection. The detector element is assumed to be a polyvinylidene difluoride (PVDF) thin pyroelectric film with opaque metal electrodes evaporated on both sides. The irradiating modulated-light intensity is assumed to be sinusoidal, written in the form

$$I(\lambda,\omega)=I_0(\lambda)\exp(i\omega t)\ , \tag{1}$$

where $\omega=2\pi f$ is the modulation angular frequency. The geometry of Fig. 1 has been considered previously[1] and the complex PPE signal response can be expressed as

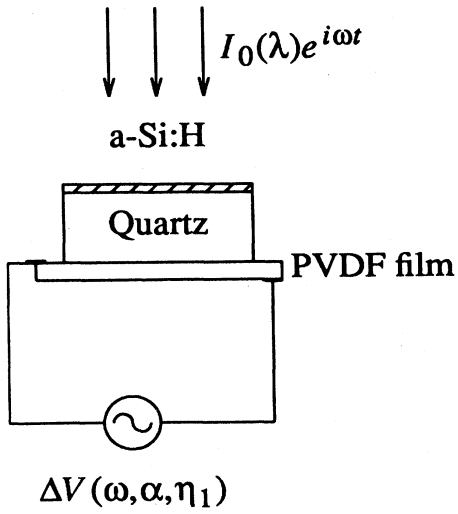

FIG. 1. Idealized PPES thin-film system geometry for theoretical considerations.

$$\Delta V \equiv S(\lambda,\omega) = C(\omega) I_0(\lambda) \times \{\eta_{Si}(\lambda) A_{Si}(\lambda) \times \exp[-(1+i) a_Q(\omega) d_Q] + A_F(\lambda)\eta_F(\lambda) T_{Si}(\lambda)\} . \quad (2)$$

In Eq. (2), $C(\omega)$ is an assortment of instrumental and geometric parameters of the sample-PVDF detector system; $\eta_{Si}(\lambda)$ and $\eta_F(\lambda)$ are the nonradiative quantum efficiencies of the a-Si:H thin film and the PVDF film detector, respectively; $A_{Si}(\lambda)$ and $T_{Si}(\lambda)$ are the Si absorptance and transmittance, respectively; and $a_Q(\omega)$ and d_Q are the thermal diffusion coefficient and thickness of the quartz substrate. The former quantity is defined by

$$a_Q(\omega) = (\omega/2\beta_Q)^{1/2} , \quad (3)$$

where β_Q is the quartz thermal diffusivity.

In the absence of the a-Si:H sample, the PPE reference signal $S_R(\lambda,\omega)$ can be written as

$$\Delta V_{ref} \equiv S_R(\lambda,\omega) = C(\omega) I_0(\lambda) \eta_F(\lambda) A_F(\lambda) . \quad (4)$$

For the present purposes, the PVDF film absorptance $A_F(\lambda)$ is

$$A_F(\lambda) \approx 1 - R_F(\lambda) , \quad (5)$$

i.e., the transmittance of the detector will be assumed to be zero, a very good approximation for electroded and coated thin-film pyroelectric PVDF. In Eq. (5) $R(\lambda)$ stands for reflectance. Two special cases of the simple theory presented above are of experimental interest in the context of this work.

A. High-frequency limit

This limit is defined by the thermally thick condition

$$a_Q(\omega) d_Q \gg 1 \quad (6)$$

or

$$f \gg \beta_Q/\pi d_Q^2 . \quad (7)$$

Equations (2) and (4) then yield the normalized signal expression

$$\frac{S(\lambda,\omega)}{S_R(\lambda,\omega)} \approx T_{Si}(\lambda) . \quad (8)$$

In this case, a wavelength scan will produce an optical transmission spectrum of the thin-film sample.

For a thin absorbing a-Si:H film deposited on a nonabsorbing substrate, at normal incidence, it is known that[11]

$$T_{Si}(\lambda) = 16 n_0 n_Q (n^2+k^2)/[BD \exp(\alpha d_{Si}) + EC \exp(-\alpha d_{Si}) + 2V \cos(4n\pi d_{Si}/\lambda) + 2U \sin(4n\pi d_{Si}/\lambda)] , \quad (9)$$

where n_0 is the index of refraction for air ($n_0 = 1$), n_Q is the quartz index of refraction ($\approx n_{glass} = 1.516$), and the a-Si:H thin-film complex refractive index is given by

$$N(\lambda) = n(\lambda) - ik(\lambda) , \quad (10)$$

with the extinction coefficient associated with the optical-absorption coefficient through the relation

$$\alpha(\lambda) = \frac{4\pi k(\lambda)}{\lambda} . \quad (11)$$

The remaining constants in Eq. (9) are defined as follows:

$$\begin{Bmatrix} B \\ C \end{Bmatrix} = (n \pm n_Q)^2 + k^2 , \quad (12)$$

$$\begin{Bmatrix} D \\ E \end{Bmatrix} = (n \pm n_0)^2 + k^2 , \quad (13)$$

$$V = (n_0^2 + n_Q^2)(n^2+k^2) - (n^2+k^2)^2 - n_0^2 n_Q^2 + 4 n_0 n_Q k^2 , \quad (14)$$

$$U = 2k(n_Q + n_0)(n^2 + k^2 - n_0 n_Q) . \quad (15)$$

Furthermore, $n(\lambda)$ and $k(\lambda)$ are linked together through Eq. (9) and a similar nonlinear expression[11] for the reflectance $R(\lambda)$. No simple mathematical method exists for solving for $n(\lambda)$ and $k(\lambda)$ from the expressions for $T(\lambda)$ and $R(\lambda)$, however, several schemes have appeared in the literature with various degrees of success.[12–15] For the purpose of obtaining approximate PPE spectra from experimental data through the optical-gap region, the mathematically convenient in-

coherent approximation[16] may be used:

$$T(\lambda)=16n^2n_0n_Q/[BD\exp(\alpha d_{Si})-CE\exp(-\alpha d_{Si})]\ . \tag{16}$$

B. Low-frequency limit

In this case the thermally thin condition

$$f\leq\beta_Q/\pi d_Q^2 \tag{17}$$

gives the following expression for the normalized signal:

$$\frac{S(\lambda,\omega)}{S_R(\lambda,\omega)}=\{\eta_{Si}(\lambda)A_{Si}(\lambda)\exp[-(1+i)a_Q(\omega)d_Q] +\eta_F(\lambda)A_F(\lambda)T_{Si}(\lambda)\}/\eta_F(\lambda)A_F(\lambda)\ . \tag{18}$$

Under the realistic assumption[1]

$$\eta_F(\lambda)\approx 1\ , \tag{19}$$

and, in view of the fact that $R_{Si}(\lambda)$ does not change by more than approximately 25% across the optical gap for a-Si:H thin films,[16,17] we set

$$A_{Si}(\lambda)=1-R_{Si}(\lambda)-T_{Si}(\lambda)\approx 1-T_{Si}(\lambda)\ . \tag{20}$$

This approximation, in practice, is not as bad as it may appear in the first place: neglecting $R_{Si}(\lambda)$ contributions for the sake of experimental PDS data interpretation has been previously used[4] successfully and has yielded optical-absorption-coefficient information within an error of less than 20%. Under these conditions, the low-frequency PPES normalized signal becomes

$$\frac{S(\lambda,\omega)}{S_R(\lambda,\omega)}\approx\eta_{Si}(\lambda)\left[\frac{1-T_{Si}(\lambda)}{A_F(\lambda)}\right]\exp[-(1+i)a_Q(\omega)d_Q] +\left[\frac{T_{Si}(\lambda)}{A_F(\lambda)}\right]\ . \tag{21}$$

III. EXPERIMENTAL AND RESULTS

a-Si:H thin films were prepared on quartz by plasma-enhanced chemical-vapor deposition (PECVD). The substrate temperature was 225 °C, the total plasma power was 40 W, and the feeding gas was SiH_4 diluted to 10% in helium. The gas-flow rate was 200 sccm (cubic cm per min at STP) and the total gas pressure was 400 mTorr. The quartz substrates had been sputtered clean in argon prior to deposition and were mounted at the anode of the PECVD system.

Figure 2 shows an outline of the PPE spectrometer. Both sample-holder and reference cells were fabricated using standard commercially available components as described elsewhere.[18] The surfaces of the 28-μm-thick PVDF films were blackened so as to minimize the film reflectance $R_F(\lambda)$, which was shown to vary substantially for Ni-Al electrodes[19] across the spectral range of interest (500–900 nm). The samples used in this work were placed on the exposed, blackened PVDF ground electrode and were held in place mechanically by use of gentle pressure so as to achieve intimate thermal contact, as

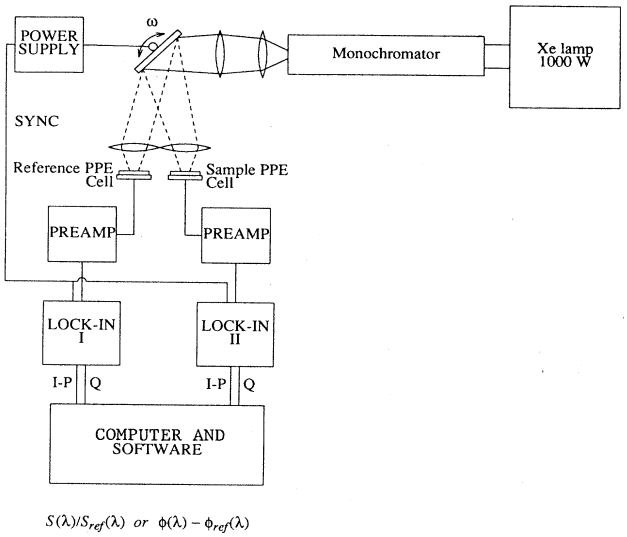

FIG. 2. Photopyroelectric spectroscopic apparatus for thin-film studies. An oscillating mirror was used as a chopper. On-line spectral normalization was effected by simple computer software.

indicated by the optimized photopyroelectric signal magnitude at low modulation frequencies (thermally thin limit). The signal quality was improved substantially by using two Ithaco 1201 low-noise preamplifiers and appropriate frequency band-pass settings before channeling the photopyroelectric signals to lock-in amplifiers. For purposes of comparison, a quartz cuvette containing an a-Si:H sample was filled with CCl_4 and held in place of the sample PVDF detector cell. A He-Ne laser probe beam was added and conventional normalized PD spectra were obtained using a standard position sensor (UDT model 431 position monitor connected to a UDT SC125 light-position detector) fitted with a narrow-band optical filter at 632.8 nm. PDS signal normalization was performed through ratioing by the reference cell PPE signal. The PDS signal quality was further enhanced using an Ithaco 1201 preamplifier stage in the same manner as with the PPES signal processing.

Figure 3 shows normalized PPE spectra obtained at 20 and 0.9 Hz. The low-energy-end interference fringe patterns essentially coincide for both frequencies, in agreement with the highly transparent nature of the sample in that region where direct optical transmission is the cause of PPE signal generation. At the high-energy end of the spectrum, transmission-related signals are only of minor importance and contribute little in the thermally thick limit (20 Hz). The major contributor to the thermally thin (0.9 Hz) signal is the transmission of the thermal wave generated within the Si film, which is acting as a heating strip on the surface of the much thicker quartz substrate.

Figures 4(a) and 4(b) show the results of using the incoherent approximation, Eq. (16), to reduce the data. Toward this end, the following steps were utilized: (a) The maximum transmittance was calculated theoretically, assuming $k(\lambda)=0$, from

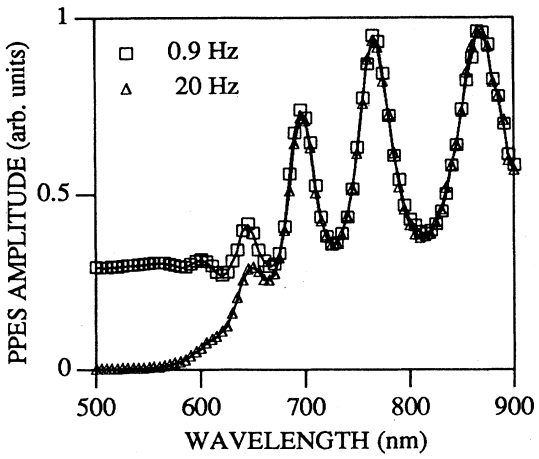

FIG. 3. PPE spectra of a-Si:H film on quartz. Slit-width resolution: 16 nm.

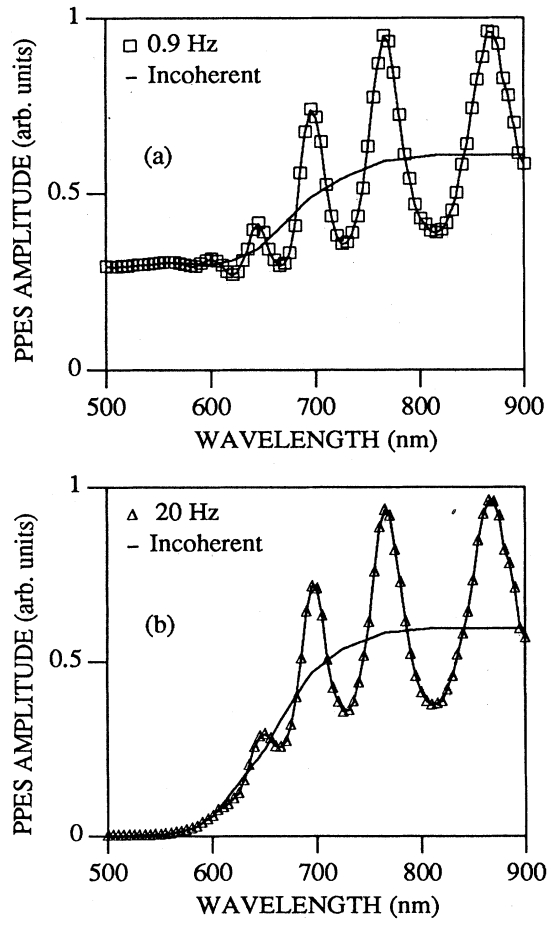

FIG. 4. Incoherent approximation calculations of PPE signals in (a) the thermally thin and (b) thermally thick cases. The curve in (b) was used as $T_{Si}(\lambda)$ in Eq. (8).

$$T_{max}=\frac{4n_0n_Q}{(n_0+n_Q)^2}=0.96\ ; \tag{22}$$

(b) the lowest-energy experimental interference fringe maximum was matched with the theoretical T_{max} at 0.96 (Fig. 3); (c) the incoherent transmission was calculated from the envelope of extrema as the geometric average[20]

$$T_I=(T_{max}T_{min})^{1/2}\ ; \tag{23}$$

(d) Eq. (16) was used in the form

$$(T_I^{max})_{theor}=\frac{4n_0n_Qn}{(n^2+n_0n_Q)(n_0+n_Q)}=(T_I^{max})_{expt} \tag{24}$$

for $k(\lambda)=\alpha(\lambda)=0$, where $(T_I^{max})_{expt}$ is the value given from the flat portion of the PPE transmission spectrum, or from the largest measured λ; (e) Eq. (24) was finally solved for n:

$$n^2=\frac{1}{2a}[-b+(b^2-4ac)^{1/2}]\ ;$$

$$a\equiv 1,\quad b\equiv-\frac{4n_0n_Q}{(n_0+n_Q)T_I^{max}},\quad c\equiv n_0n_Q\ . \tag{25}$$

Using $T_I^{max}=0.596$, Eq. (25) yields $n=3.61$. This value for n is well within the band of accepted values for a-Si:H thin films.[6,21] It was assumed spectrally constant (also a standard thin-film PDS assumption[4]), and was subsequently used in all further calculations. The incoherent curves of Fig. 4 were thus obtained using $n=3.61$. Figure 5 shows the optical-absorption-coefficient $\alpha(\lambda)$ spectrum obtained using the incoherent approximation of Fig. 4(b) as $T_{Si}(\lambda)$ in Eqs. (8) and (16). The values for $\alpha(\lambda)$ were obtained using the numerical method of halving the interval (or bisection method).[2] For these calculations, the a-Si:H thin-film thickness was estimated from the interference pattern of Fig. 3 using the approximate formula ($n=$const)[23]

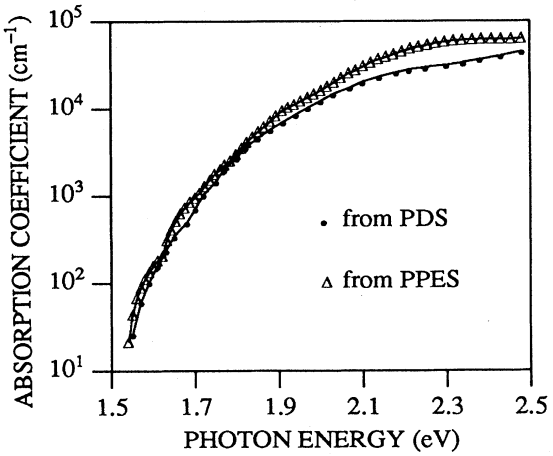

FIG. 5. Optical-absorption-coefficient calculation for a-Si:H thin film using PPES and PDS. For details, see text.

$$d_{\mathrm{Si}}=\frac{1}{2n}\left[\frac{\lambda_{m+1}\lambda_m}{\lambda_{m+1}-\lambda_m}\right]\approx 0.9\ \mu\mathrm{m}\ , \tag{26}$$

where λ_{m+1},λ_m correspond to adjacent interference maxima such that $\lambda_{m+1}>\lambda_m$. Figure 5 also shows the $\alpha(\lambda)$ spectrum obtained using conventional PDS. Assuming complete photothermal saturation at 500 nm, the normalized PDS signal may be divided by its saturation value, yielding[24]

$$I_{\mathrm{PDS}}(\lambda)/I_{\mathrm{PDS}}(\lambda_{\mathrm{saturation}}) = \left[\frac{\eta_{\mathrm{Si}}(\lambda)}{\eta_{\mathrm{Si}}(\lambda_{\mathrm{saturation}})}\right]\{1-\exp[-\alpha(\lambda)d_{\mathrm{Si}}]\}\ . \tag{27}$$

The PD $\alpha(\lambda)$ spectrum of Fig. 5 was obtained by smoothing the raw PDS signal output to eliminate the interference fringes, using a three-point averaging technique which was found very useful in previous work.[25] In addition, the simplifying assumption $\eta_{\mathrm{Si}}(\lambda)/\eta_{\mathrm{Si}}(\lambda_{\mathrm{saturation}})=1$ was made, in line with conventional PDS spectroscopic calculations of thin films.[4] The similarity of the two entirely independently obtained $\alpha(\lambda)$ curves in Fig. 5 is remarkable and is a proof of the good spectroscopic capabilities of both techniques in measuring optical absorption. Figure 5 shows that the assumption of saturation at $\lambda=500$ nm is justified, in retrospect, as $1-\exp[-\alpha(500\mathrm{nm})d_{\mathrm{Si}}]\approx 1-\exp(-7)\approx 1$. It ought to be noticed, however, that the PDS absorption curve falls consistently under the PPES curve throughout the measured spectral region. It will be seen below that the most likely source of this discrepancy is the nonconstancy of $\eta_{\mathrm{Si}}(\lambda)$.

The incoherent curve in Fig. 4(a) was then used for the self-consistent calculation of the nonradiative quantum efficiency $\eta_{\mathrm{Si}}(\lambda)$. In view of the blackened PVDF detector surfaces,

$$A_F(\lambda)\approx 1\ , \tag{28}$$

to a very good approximation, so that Eq. (21) may be further simplified:

$$\frac{S(\lambda,\omega)}{S_R(\lambda,\omega)}\approx\eta_{\mathrm{Si}}(\lambda)[1-T_{\mathrm{Si}}(\lambda)] \times\exp[-(1+i)a_Q(\omega)d_Q]+T_{\mathrm{Si}}(\lambda)\ . \tag{29}$$

Now, the thermally thin limit equation (29) indicates that, given experimental values for $T_{\mathrm{Si}}(\lambda)$ (high-frequency PPES signal at incoherent approximation), and a good knowledge of d_Q and $a_Q(\omega)$, $\eta_{\mathrm{Si}}(\lambda)$ may be calculated self-consistently for each wavelength using the amplitude of the low-frequency PPES signal. Figure 6 shows the frequency dependence of the PPES signal in the opaque region ($\lambda=490$ nm). In that region $1-T_{\mathrm{Si}}(\lambda)\approx 1$ in Eq. (29) and one obtains

$$\ln\left|\frac{S(\lambda,\omega)}{S_R(\lambda,\omega)}\right|\approx -a_Q(\omega)d_Q\ . \tag{30}$$

A measurement of the slope of the line in Fig. 6 and use of Eq. (3) yielded the value $\beta_Q=7.85\times10^{-3}$ cm^2/s

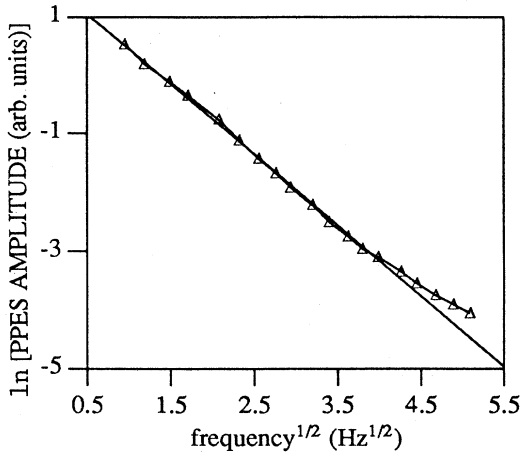

FIG. 6. Frequency dependence of normalized PPES signal from a-Si:H system in the opaque spectral region ($\lambda=490$ nm).

for the quartz thermal diffusivity, in good agreement with published values.[26] Finally, Eq. (29) was solved for $\eta_{\mathrm{Si}}(\lambda)$ in the form

$$\eta_{\mathrm{Si}}(\lambda)=\frac{1}{1-T_{\mathrm{Si}}(\lambda)}\exp(a_Q d_Q) \times\left[\left|\left|\frac{S(\lambda,\omega)}{S_R(\lambda,\omega)}\right|^2-T_{\mathrm{Si}}^2(\lambda)\sin^2(a_Q d_Q)\right]^{1/2} -\cos(a_Q d_Q)\right]\ . \tag{31}$$

The resulting $\eta_{\mathrm{Si}}(\lambda)$ spectrum is shown in Fig. (7). The nonradiative quantum efficiency of the a-Si:H thin-film sample is seen to vary by more than 1 order of magnitude across the material optical gap. It saturates at wavelengths above the gap, becoming independent of $h\nu$, as reported elsewhere,[6] and decreases for below-the-gap excitation, in agreement with indirect (photoluminescence) measurements performed previously.[27,28] Thermal conversion efficiencies in the 0.5–0.001 range were previously determined photoacoustically[5] for Ge-doped As_2Se_3 chalcogenide glasses, with order-of-magnitude variations across the optical-absorption gap. No similar spectral dependencies for a-Si:H thin-film semiconductors have been reported in the literature, to the authors' best knowledge, for direct comparisons with the spectrum of Fig. 7. The increase in $\eta_{\mathrm{Si}}(\lambda)$ for $\lambda\geq 720$ nm is not entirely understood at this time; however, it is associated with the cusp in the PPE $\alpha(\lambda)$ curve at the same wavelength in Fig. 5. Figure 7 indicates that the PDS assumption that $\eta_{\mathrm{Si}}(\lambda)\approx\eta_{\mathrm{Si}}(\lambda_{\mathrm{saturation}})$ is not valid, and the fact that $\eta_{\mathrm{Si}}(\lambda)<1$ throughout the spectral range of interest is responsible for the lower effective absorption-coefficient values calculated via PDS.

IV. DISCUSSION

The PPE optical-absorption-coefficient data of Fig. 5 may be understood largely in terms of amorphous Si

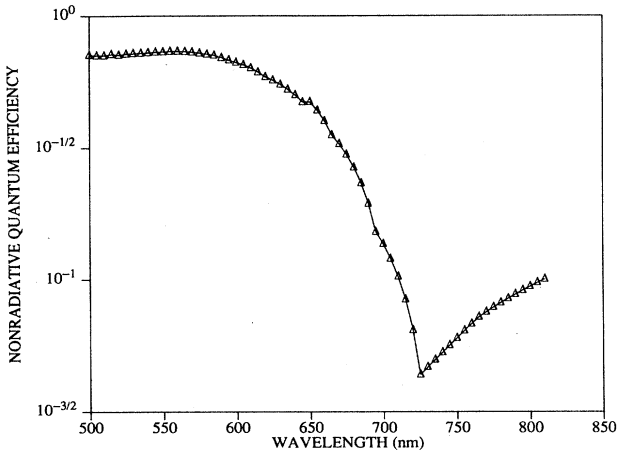

FIG. 7. Nonradiative quantum efficiency spectrum of a-Si:H thin film.

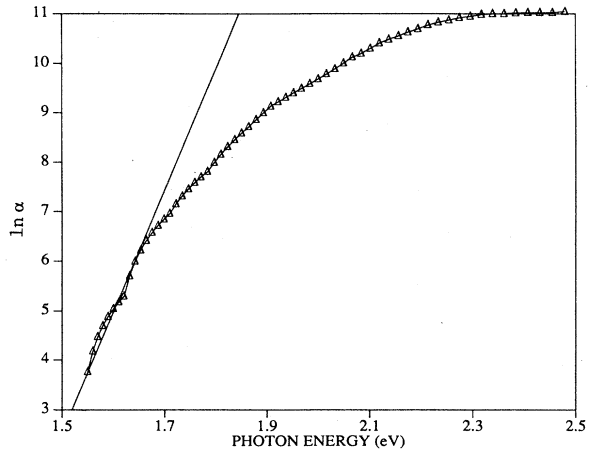

FIG. 9. Optical-absorption-coefficient PPE spectrum plotted to illustrate the $\ln\alpha$ dependence on $h\nu$.

thin-film physics. Assuming a parabolic conduction-band density-of-states approximation for nondirect optical transitions (i.e., a constant dipole-interaction matrix element), the behavior of the optical-absorption coefficient is given by[29]

$$\alpha(h\nu) \propto (h\nu - E_G)^2 / n(h\nu) h\nu \ , \tag{32}$$

where E_G is the characteristic energy of the distribution of electronic states in bandlike regions (i.e., the optical gap). Figure 8 shows the appropriately plotted data and an estimated $E_G = 1.7$ eV from the intercept of the (least-squares-fitted) straight line to the data. This value of E_G is well within the spread of previously reported values:[16] 1.6–1.7 eV.

The low-energy tail of the spectrum in Fig. 5 may also be explained in terms of an exponential valence-band density-of-states (Urbach tail) approximation:[29]

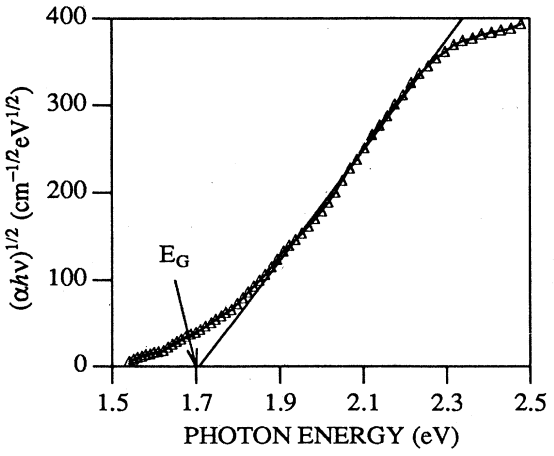

FIG. 8. Optical-absorption-coefficient PPE spectrum plotted to illustrate the $(\alpha h\nu)^{1/2}$ dependence on $h\nu$.

$$\alpha(h\nu) \propto \exp(h\nu / E_0) \ , \tag{33}$$

where E_0 is the characteristic energy of the distribution of electronic states in the tail-like region. Plotting the PPES data as shown in Fig. 9 and calculating the slope, one finds the value $E_0 \approx 41$ meV. This value is also well within the spread of previously reported values:[16] 25–80 meV. The good agreement of the absorption-tail PPE-signal-derived E_0 value with an Urbach-tail interpretation, i.e., a disorder-induced tailing off of defect states into the optical gap,[30] is consistent with the increase in the nonradiative quantum efficiency in that region, Fig. 7: the disordered nature of the subgap defect states in the a-Si:H thin-film sample is expected to show enhanced optical-to-thermal energy-conversion activity. Such defects have previously been hypothesized to be the cause of luminescence quenching.[31] The direct $\eta_{Si}(\lambda)$ evidence provided in this work indicates, in agreement with this hypothesis, that the preferred subgap deexcitation channel is increasingly nonradiative, at the expense of other energy-transfer processes, such as the strong room-temperature defect luminescence reported previously.[28] Clearly, more work is needed to fully understand the implications of the subgap spectral dependence of $\eta_{Si}(\lambda)$ in Fig. 7. PPES appears to be a photothermal technique capable of producing *direct* $\eta(\lambda)$ spectra for the first time. This capability is expected to be an important vehicle to study in detail nonradiative deexcitation physics of amorphous semiconducting thin films.

V. CONCLUSIONS

In this work, PPES was shown to be capable of providing a-Si:H thin-film $\alpha(\lambda)$ and $\eta(\lambda)$ spectra directly and self-consistently from measurements at two modulation frequencies (thermally thick and thermally thin limits). Comparison of PPES $\alpha(\lambda)$ spectra with conventional PDS-obtained data showed that both techniques yield high-quality results; however, PDS-extracted values tend to be underestimates, due to nonunity values for $\eta(\lambda)$. Therefore, PPES appears to be very promising for amor-

phous thin-film work. Its main advantages over conventional PDS are (a) the absence of the solid-liquid interface, which is an undesirable feature for the characterization of optoelectronically active surfaces, and (b) the direct spectroscopic measurement of the nonradiative quantum efficiency, an important quantity for the quality control and characterization of optoelectronic materials and devices.

ACKNOWLEDGMENTS

This work was supported by the Ontario Laser and Lightwave Research Center and the Natural Sciences and Engineering Research Council (NSERC) of Canada. The assistance of Linda Gowman and Gordon Verdin during the early stages of this work are gratefully acknowledged.

[1]H. Coufal, Appl. Phys. Lett. **45**, 516 (1984).
[2]K. Tanaka, in *Photoacoustic and Thermal Wave Phenomena in Semiconductors,* edited by A. Mandelis (North-Holland, New York, 1987), Chap. 16; K. Tanaka, Y. Ichimura, and K. Sindoh, J. Appl. Phys. **63**, 1815 (1988).
[3]A. Mandelis and M. M. Zver, J. Appl. Phys. **57**, 4421 (1985).
[4]N. M. Amer and W. B. Jackson, in *Semiconductors and Semimetals,* edited by J. I. Pankove (Academic, New York, 1984), Vol. 21B, Chap. 3.
[5]M. Kitamura, T. Ogawa, and T. Arai, J. Phys. Soc. Jpn. **52**, 2561 (1983).
[6]S. Yamasaki, Philos. Mag. B **56**, 79 (1987).
[7]A. F. S. Penna, J. Shah, A. E. DiGiovanni, A. Y. Cho, and A. C. Gossard, Appl. Phys. Lett. **47**, 591 (1985).
[8]J. D. Winefordner and M. Rutledge, Appl. Spectrosc. **39**, 377 (1985).
[9]W. B. Jackson, N. M. Amer, A. C. Boccara, and D. Fournier, Appl. Opt. **20**, 1333 (1981).
[10]L. C. Aamodt and J. C. Murphy, J. Appl. Phys. **52**, 4903 (1981).
[11]F. Abelès, in *Advanced Optical Techniques,* edited by A. C. S. van Heel (North-Holland, Amsterdam, 1967), Chap. 5.
[12]R. E. Denton, R. D. Campbell, and S. G. Tomlin, J. Phys. D **5**, 852 (1972).
[13]J. C. Manifacier, J. Gasiot, and J. P. Fillard, J. Phys. E **9**, 1002 (1976).
[14]T. C. Paulick, Appl. Opt. **25**, 562 (1986).
[15]K. A. Epstein, D. K. Misemer, and G. D. Vernstrom, Appl. Opt. **26**, 294 (1987).
[16]G. D. Cody, in *Semiconductors and Semimetals,* edited by J. I. Pankove (Academic, New York, 1984), Vol. 21B, Chap. 2.
[17]D. T. Pierce and W. E. Spicer, Phys. Rev. B **5**, 3017 (1972).
[18]H. J. Coufal, R. K. Grygier, D. E. Horne, and J. E. Fromm, J. Vac. Sci. Technol. A **5**, 2875 (1987).
[19]PVDF Kynar^R film with standard Ni-Al electrodes was purchased from Pennwalt Corp., Piezo Film Dept., 950 Forge Avenue, Valley Forge, PA 19482.
[20]K. Driss-Khodja, A. Gheorghiu, and M.-L. Theye, Opt. Commun. **55**, 169 (1985).
[21]S. K. Bahl and S. M. Bhagat, J. Non-Cryst. Solids **17**, 409 (1975).
[22]C. F. Gerald, *Applied Numerical Analysis,* 2nd ed. (Addison-Wesley, Reading, MA, 1980), p. 3.
[23]A. Mandelis, E. K. M. Siu, and S. Ho, Appl. Phys. A **33**, 153 (1984).
[24]A. Mandelis, J. Appl. Phys. **54**, 3404 (1983).
[25]T. Dioszeghy and A. Mandelis, J. Phys. Chem. Solids **47**, 1115 (1986); D. D. McCracken and W. S. Dorn, *Numerical Methods and FORTRAN Programming* (Wiley, New York, 1964).
[26]A. C. Bento, H. Vargas, M. M. F. Aguiar, and L. C. M. Miranda, Phys. Chem. Glasses **29**, 127 (1987).
[27]R. A. Street, Phys. Rev. B **21**, 5775 (1980).
[28]M. Tajima, H. Okushi, S. Yamasaki, and K. Tanaka, Phys. Rev. B **33**, 8522 (1986).
[29]M. H. Brodsky, R. S. Title, K. Weiser, and G. D. Pettit, Phys. Rev. B **1**, 2632 (1970).
[30]N. F. Mott, Adv. Phys. **16**, 49 (1967).
[31]W. B. Jackson and N. M. Amer, Phys. Rev. B **25**, 5559 (1982).